Earth and Planetary Science Letters, 115 (1993) 257–273
Elsevier Science Publishers B.V., Amsterdam

[DT]

Diagenetic formation of ferrimagnetic iron sulphide minerals in rapidly deposited marine sediments, South Island, New Zealand

Andrew P. Roberts [1] and Gillian M. Turner

Institute of Geophysics, Research School of Earth Sciences, Victoria University of Wellington, P.O. Box 600, Wellington, New Zealand

Received May 10, 1992; revision accepted January 4, 1993

ABSTRACT

Detailed magnetostratigraphic studies of Late Neogene siliciclastic sediments of the Awatere Group, South Island, New Zealand (41°45'S, 174°05'E) have revealed a wide range of palaeomagnetic behaviour. Examination of rock magnetic properties was undertaken using conventional palaeomagnetic techniques and thermomagnetic, X-ray diffraction and electron microprobe analyses. These analyses indicate that the ferrimagnetic iron sulphide minerals, greigite and pyrrhotite, are responsible for a stable and intense magnetic remanence in fine-grained sediments, whereas titanomagnetite is the only remanence-bearing mineral identified in coarser-grained sediments, which are less strongly and less stably magnetised than the fine-grained sediments. Detrital titanomagnetite grains are likely to have undergone dissolution during early diagenesis as a result of iron sulphide formation, which occurs commonly in rapidly deposited, anoxic sediments that support active sulphate reduction and H_2S formation. Preservation of greigite and pyrrhotite is inferred to result from the arrest of the pyritisation process, probably due to the low permeability of the fine-grained sediments and consumption of available H_2S before full reaction to pyrite occurred. Relative palaeomagnetic instability and weak remanence intensities in coarser grained sediments is likely to be due to low titanomagnetite concentrations resulting from titanomagnetite dissolution.

1. Introduction

Post-depositional detrital remanent magnetisation (pDRM) is now generally believed to be the dominant process involved in the magnetisation of sediments prior to diagenesis [1]. Post-depositional formation of authigenic magnetic minerals and diagenetic alteration of primary remanence carriers are also recognised as fundamental aspects of sedimentary palaeomagnetism [2]. Nevertheless, relatively little is known about the diagenetic processes that affect the magnetic signature in marine sediments despite the enormous amount of palaeomagnetic research undertaken in such sediments.

Many thick sequences of rapidly deposited Neogene marine sediments in New Zealand have been uplifted and are now exposed above sea level. Several pioneering land-based magnetostratigraphic studies were made in such successions in New Zealand [3–5], as well as numerous recent studies [6–11]. The rock magnetic properties of these sediments are, however, still not well understood.

A rock magnetic study of a thick succession of siliciclastic marine sediments of Late Miocene to Early Pliocene age (Awatere Group), exposed by Blind River and Upton Brook in the Lower Awatere Valley, northeastern South Island, New Zealand (Fig. 1) is presented here. Magnetostratigraphic studies of Awatere Group sediments indicate that they were deposited rapidly at rates varying between 0.3 and 1.0 m/k.y. [5,8,10]. In these studies, it was observed that fine-grained sediments (mudstones) are generally intensely and stably magnetised and that coarser grained sediments (siltstones and sandstones) are relatively weakly and less stably magnetised [10].

[1] Present address: Department of Geology, University of California, Davis, CA 95616, USA.

This rock magnetic investigation was carried out to determine the relationship between magnetic minerals, sediment grain size and palaeomagnetic behaviour. This paper is the first to relate the complex palaeomagnetic behaviour observed in the much-studied New Zealand sediments to the magnetic minerals present, and the diagenetic processes that have affected the sediments.

2. Geological setting

The sediments of the Awatere Group rest unconformably on siliciclastic Mesozoic rocks of the Torlesse Supergroup (Fig. 1) and are clearly derived from them. Awatere Group sediments contain small amounts of heavy minerals such as titaniferous iron oxides, biotite and Cr spinel [10], which are rare in Torlesse rocks [12]. It is therefore likely that the Awatere Group is also derived from igneous sources in central Marlborough (Fig. 1) which are rich in such minerals [13].

Facies types of correlative sediment in the Awatere Group vary laterally due to changes in depth of deposition and proximity to sediment source [14]. Sediments exposed at Upton Brook were deposited at shallower water depths than those at Blind River [14], and greater lithological variation exists at Upton Brook. Stratigraphic columns and sampling sites are shown in Fig. 2. We have examined the rock magnetism of sediments at Upton Brook in greater detail because of the lithological variation at that locality.

3. Sampling and laboratory procedures

Conventional palaeomagnetic cores (25 mm in diameter) were collected at stratigraphic intervals of ca. 5 m for magnetostratigraphic studies at

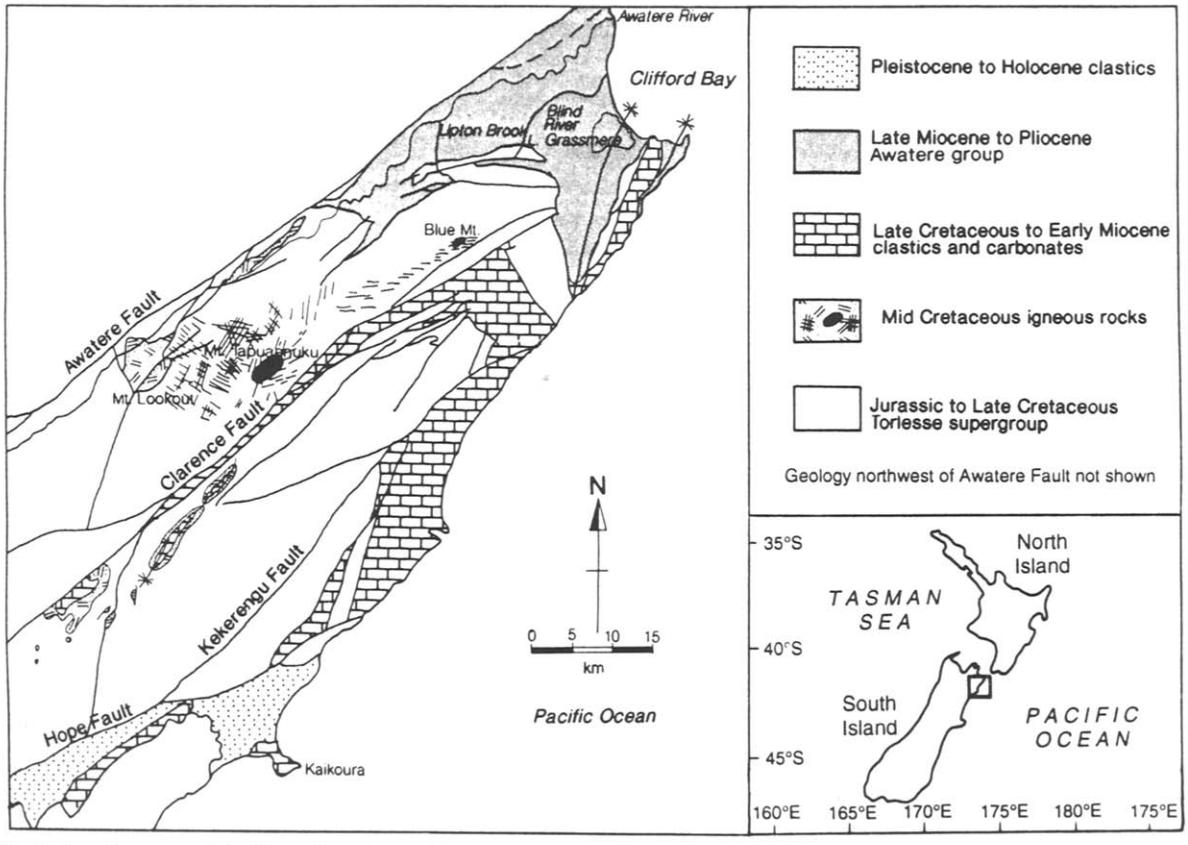

Fig. 1. Location map of the Upton Brook and Blind River successions, and generalised geological map showing distribution of the Awatere Group, Torlesse Supergroup and igneous rocks in Marlborough region, South Island, New Zealand.

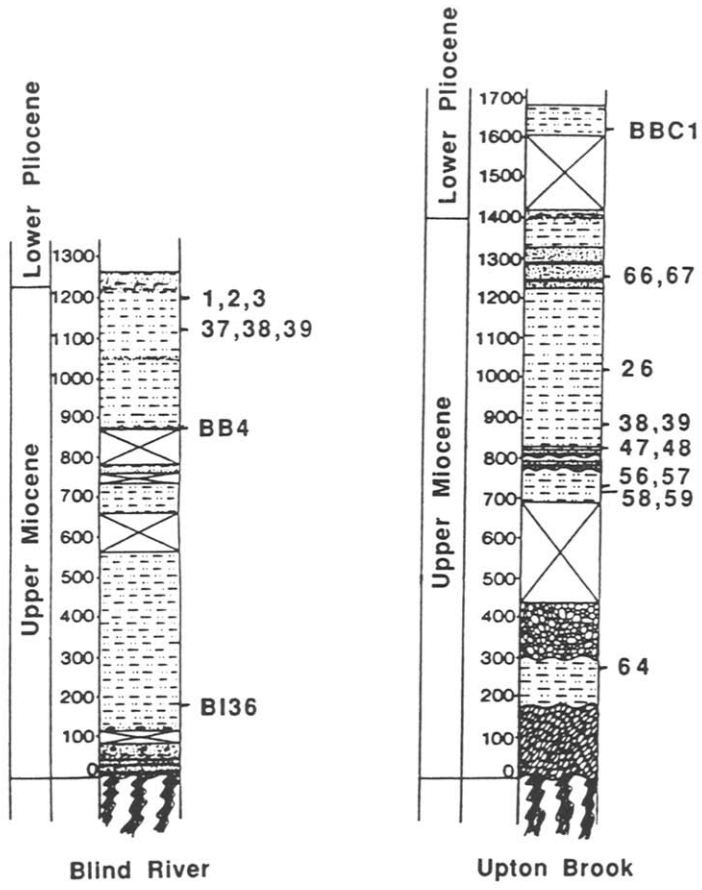

Fig. 2. Stratigraphic succession and location of sites sampled at Blind River and Upton Brook for this study.

Blind River and Upton Brook [8,10]. All cores were stored in mu-metal shields from the time of sampling until measurement. Cores were cut into 22 mm samples in the laboratory and were stored in mu-metal shields until dry.

Measurements of magnetic remanence were made on a two-axis ScT superconducting rock magnetometer. Stepwise thermal demagnetisation was the only demagnetisation treatment used because previous experience with similar mudstones from New Zealand has shown that thermal demagnetisation is generally much more effective than alternating field demagnetisation in isolating the characteristic component of remanence [5,7–11]. Demagnetisation temperatures of 100, 150, 200, 250, 300 and 350°C were used routinely, with additional intermediate steps in some cases. Thermal alteration and growth of secondary magnetic minerals usually occurs at temperatures of around 300–350°C. Magnetic susceptibility was measured after each heating step to monitor for thermal alteration, and further heating was terminated when the first significant changes were noted. Magnetic susceptibility measurements were made using a Bartington Instruments MS1 susceptibility meter. An isothermal remanent magnetisation (IRM) was imparted to selected samples at progressively increasing fields up to 800 mT using a Molspin pulse magnetiser. The remanence acquired at each step was measured on a Molspin spinner magnetometer. Once saturated, samples were demagnetised by applying back fields at 10 mT increments to determine the remanent coercivity, B_{cr}, the back field required to reduce the IRM from saturation to zero.

Further magnetic measurements and chemical analyses were made on magnetic separates from twelve sites, or groups of sites, from Blind River

and Upton Brook. Magnetic separates were made by crushing six or seven palaeomagnetic samples into a fine powder, suspending the powder in solution, and pumping the slurry between the poles of an electromagnet by means of a peristaltic pump, following the method of Papamarinopoulos et al. [15]. Clay minerals were deflocculated from the magnetic particles by ultrasonic treatment. Purer separates were then obtained by repeating the procedure to remove as much of the clay component as possible. The separates were dried in a gentle heat (60°C). Some workers use inert solvents and atmospheres during extraction to avoid the possibility of mineralogical alteration during the extraction process [16,17]. While magnetic separation in water may not be ideal, any mineral that is altered by water would be incapable of carrying the stable remanences observed in this study, given that these sediments have been water saturated since deposition. Similarly, any mineral that is altered by drying to temperatures of 60°C would be incapable of carrying a remanence that is stable at temperatures exceeding 300°C.

X-ray diffraction (XRD) was carried out on a Philips PW 2272/20 X-ray diffractometer with a Cu_{α} source. Electron probe microanalysis (EPMA) was carried out with a JEOL 733 Superprobe on polished thin sections of grains from four magnetic separates. Iron sulphide framboids are ubiquitous in sieved coarse (> 63 μm) fractions of Awatere Group sediments. Hand-picked iron sulphide framboids and magnetically separated iron oxide grains were analysed by EPMA in order to precisely determine their stoichiometry.

Thermomagnetic analyses were carried out on powdered magnetic separates using a Curie balance at the C.F.R. palaeomagnetic laboratory, Gif-sur-Yvette, France. Separates were heated at a rate of 10°C/min and the saturation magnetisation, M_s, was measured at every 2°C increment up to 650°C. Similarly, M_s was also measured at every 2°C drop in temperature as the separate was cooled at a rate of 10°C/min.

4. Results

4.1. Palaeomagnetic behaviour

Three types of palaeomagnetic behaviour (A, B and C) were observed in a detailed magne-

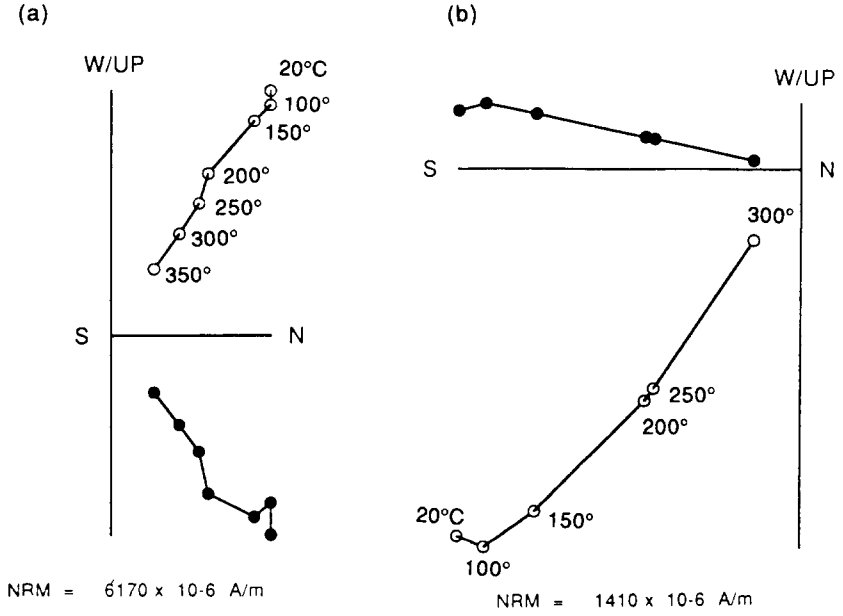

Fig. 3. Vector component diagrams showing stepwise thermal demagnetisation behaviour of samples from Upton Brook sites (a) 56 (normal polarity) and (b) 39 (reversed polarity). Dots denote projections onto the horizontal plane and circles denote projections onto the vertical plane.

tostratigraphic study that involved full stepwise thermal demagnetisation of ca. 800 samples from ca. 130 sampling sites at Upton Brook and Blind River [10]. Intense, stable remanences that are directed to the origin of vector component plots are observed from type A samples (Fig. 3). Type B samples are relatively weakly magnetised and are more heavily overprinted than type A samples. Characteristic remanences are usually not isolated before thermal alteration occurs at 300–350°C. Type C samples are generally unstably magnetised and no useful palaeomagnetic data can be retrieved. Fine-grained mudstones usually display type A behaviour, while relatively coarser grained siltstones and sandstones more frequently display behaviour of types B and C.

4.2. X-ray diffraction

Ten powdered magnetic separates were analysed by XRD. In all cases, the diffractions from magnetic minerals were masked by large peaks resulting from chlorite and quartz. Likely magnetic carriers were identified in only a few separates because of low concentrations of magnetic minerals and the difficulty in obtaining sufficiently pure separates. The results from each separate are summarised in Table 1, where iron-bearing minerals are categorised in two ways: Diffraction peaks that can be unambiguously matched with those from pure crystalline samples are denoted as "definite" matches. Minerals with less certain matches, due to low concentrations of the mineral, or to masking of some peaks by other minerals, are denoted as "probable."

Ilmenite ($FeTiO_3$) and ulvospinel (Fe_2TiO_4) have been identified in separates from several sites at Blind River and Upton Brook. Pure ilmenite and ulvospinel are paramagnetic at room temperature [18] and should not contribute to the remanence in these rocks. Maghaemite (γFe_2O_3) is likely to be the remanence carrier at site BBC1. Pyrrhotite (Fe_7S_8) and greigite (Fe_3S_4) are the most likely remanence carriers identified by XRD at sites UB 47 & 48 and UB 56 & 57, respectively. No minerals that are likely to carry a stable magnetic remanence have been identified by XRD at Blind River (Table 1).

4.3. Electron probe microanalysis

Four magnetic separates and three sets of hand-picked iron sulphide framboids from sieved coarse sediment fractions were subjected to EPMA. Oxide abundances were determined for Si, Al, Ti, Fe, Mg, Mn, Ca, Cr and Ni. A large number of paramagnetic minerals were identified, including garnet, sphene, chrome spinel, plagioclase, pyroxene, amphibole, chlorite and ilmenite. Distributions of minerals within the Fe-Ti oxide ternary system were calculated using the method of Stormer [19] and are plotted in Fig. 4. By far the greatest number of analyses are of ilmenite, the remainder being titaniferous magnetites with varying Ti contents. Variations away

TABLE 1

Minerals identified in powdered magnetic extracts by X-ray diffractometry

Site	Common minerals	Definite	Probable
Upton Brook			
BBC1	Chlorite, quartz	Ilmenite	Maghaemite, ulvospinel
UB 38 & 39	Chlorite, quartz	No other positive identifications	
UB 47 & 48	Chlorite, quartz	Ilmenite, pyrrhotite	
UB 56 & 57	Chlorite, quartz	Greigite	
UB 58 & 59	Chlorite, quartz	No other positive identifications	
UB 64	Chlorite		Ulvospinel
Blind River			
BL 1, 2 & 3	Chlorite, quartz	Ilmenite	Ulvospinel
BL 37, 38 & 39	Chlorite, quartz	Ilmenite	Ulvospinel
BB 4	Chlorite	Ilmenite	Ulvospinel
BI 36	Chlorite, quartz	Ilmenite	Ulvospinel

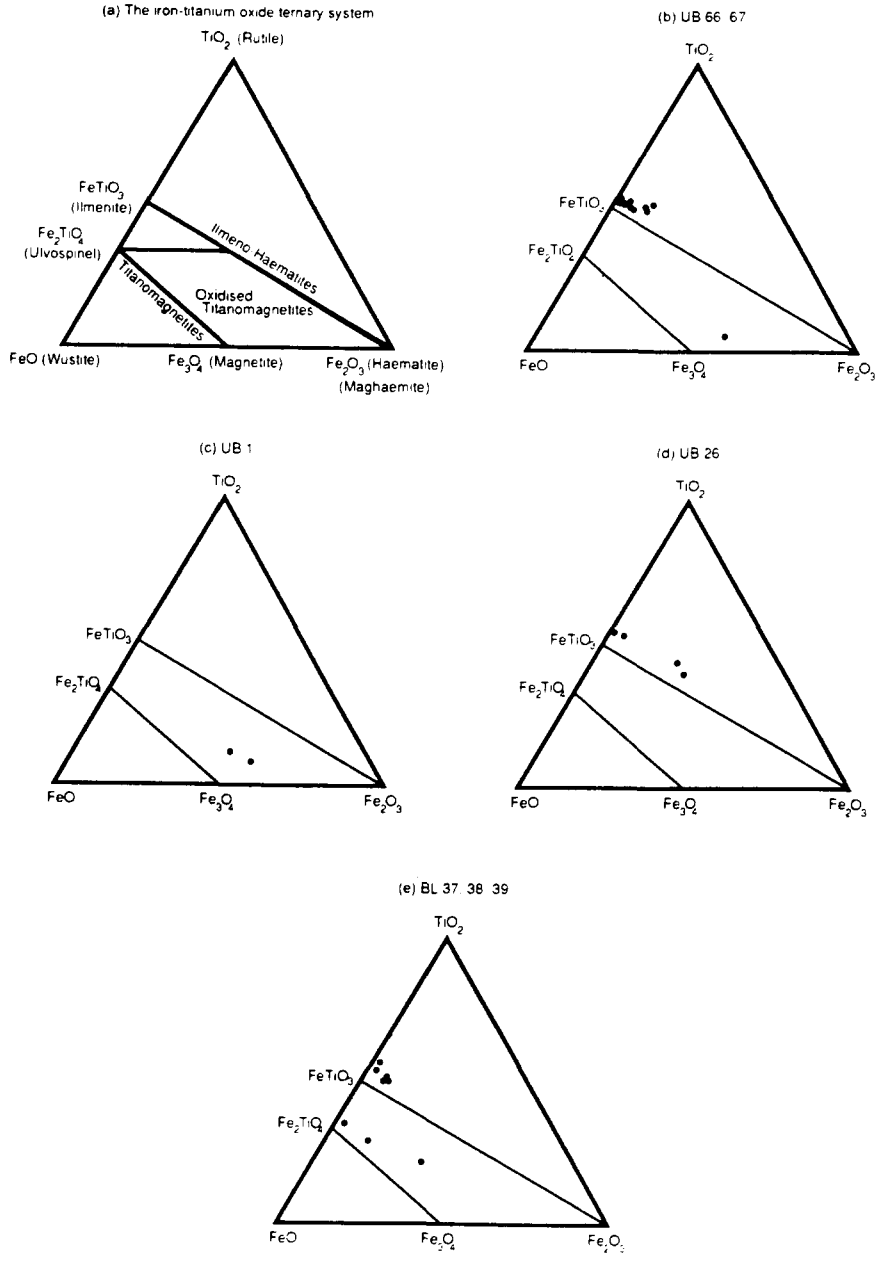

Fig. 4. The Fe-Ti oxide ternary system with distributions plotted for the compositions of individual grains analysed by electron probe microanalysis. Compositions were determined using the method of Stormer [19].

from the titanomagnetite ($Fe_{3-x}TiO_4$) and ilmeno-haematite ($Fe_{2-y}Ti_yO_3$) solid solution lines in Fig. 4 can be attributed to analytical error, variable degree of oxidation or non-stoichiometry of the mineral phases analysed. The high proportion of ilmenite in these separates is consistent with the XRD results. Analyses from sites BL 37, 38 & 39 have high Ti (ulvospinel) contents (Fig. 4e), which is also consistent with the XRD results.

The few titanomagnetite analyses reveal variable Ti contents and variable degrees of oxidation. The Curie temperatures expected for the three titanomagnetite grains, with compositions

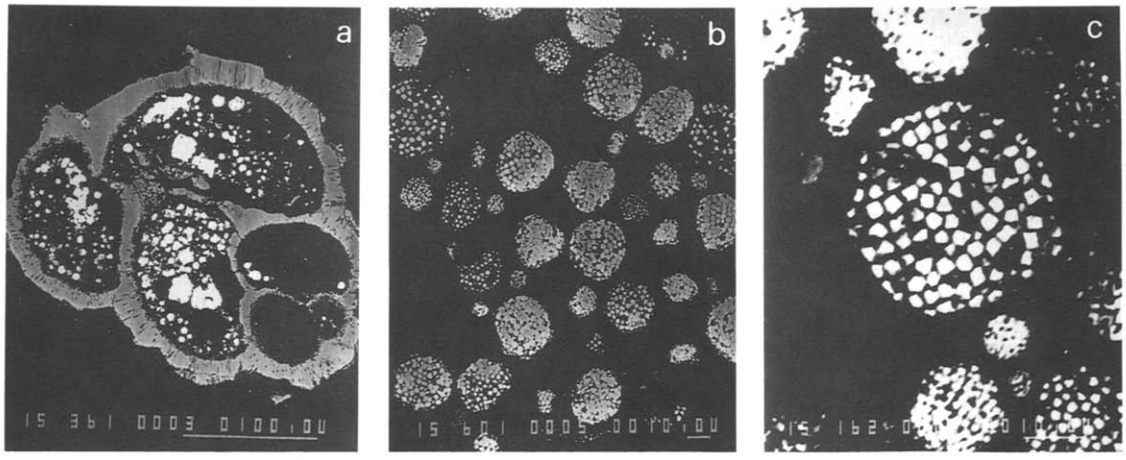

Fig. 5. (a) Back-scattered electron micrograph of thin section through foraminifer enclosing bright framboidal pyrite (scale bar 100 μm). (b) and (c) Framboidal aggregates (within foraminifer) under progressive magnification with individual pyrite crystals clearly visible (scale bar 10 μm).

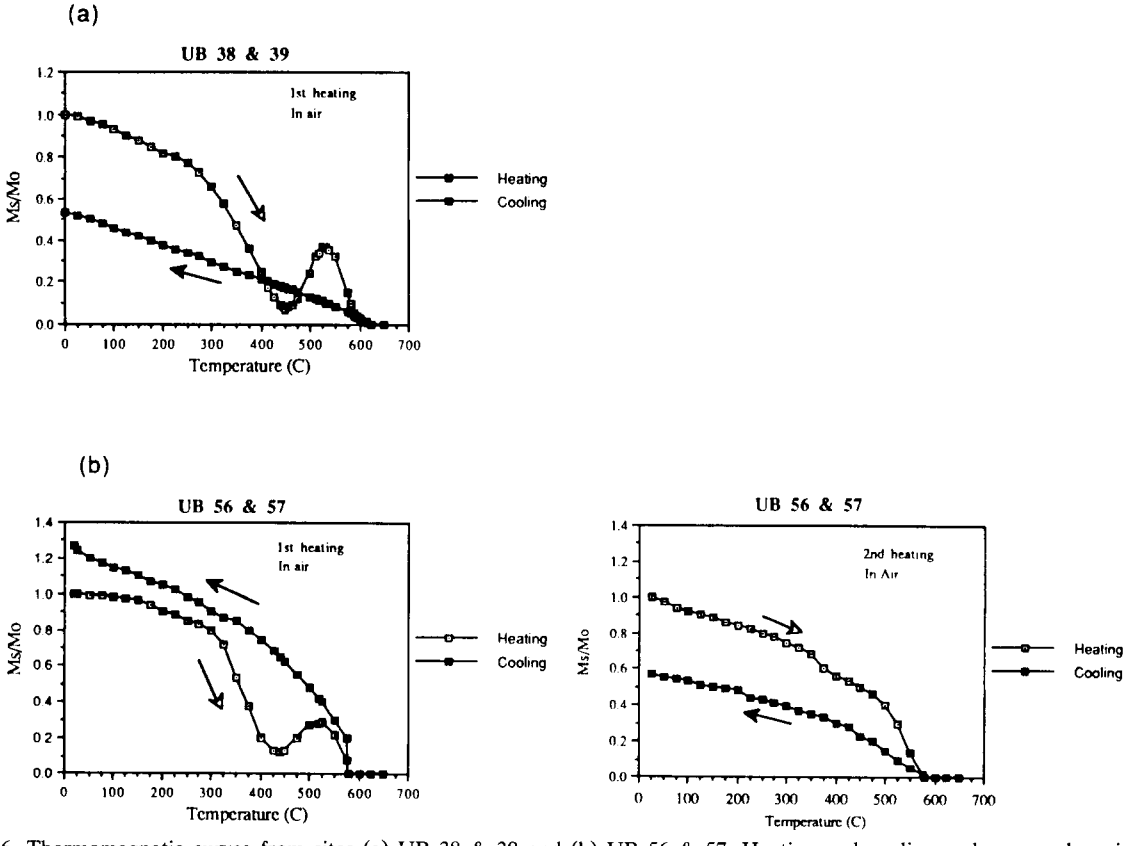

Fig. 6. Thermomagnetic curves from sites (a) UB 38 & 39 and (b) UB 56 & 57. Heating and cooling cycles were done in air (see text).

of $x = 0.16–0.31$ from sites UB 66 & 67 and UB 1 (Fig. 4b and c), range between 450 and 560°C [20]. The single titanomagnetite grain identified from sites BL 37, 38 & 39 ($x = 0.54$; Fig. 4e) would be expected to have a Curie temperature of ca. 350°C [20]. The above compositions and expected Curie temperatures suggest that titanomagnetite grains may be responsible for the magnetic remanence recorded at these sites, and that thermal alteration observed between 300 and 350°C masks any higher temperature signal.

Coarse aggregates of hand-picked iron sulphide crystals were also analysed. The term "framboid" is used to describe the raspberry-like aggregates that consist of spherical to subspherical, micrometre to sub-micrometre sized iron sulphide crystals (usually pyrite) that are contiguous but not interpenetrant [21]. Framboidal sulphide minerals are commonly associated with microfauna and are ubiquitous in the coarse sediment fractions (> 63 μm) of sieved fine-grained sediments of the Awatere Group [10].

Initially, fresh, untarnished framboidal sulphides were extracted from three coarse sediment fractions from Upton Brook (UB sites 1, 61 and 65). Micrographs of a polished section through a foraminifer enclosing framboids are shown in Fig. 5. A pyrite (FeS_2) stoichiometry was determined for all samples analysed. Pure pyrite is paramagnetic and does not contribute to magnetic remanence at room temperature.

We also attempted to analyse framboids that are tarnished by a black coating and are more strongly attracted to a hand-held magnet than the brassy yellow pyrite framboids. These framboids are not as hard as the pyrite framboids and attempts to obtain polished petrological thin sections failed. Such framboids may be ferrimagnetic and may coexist in sedimentary environments with the more common paramagnetic pyrite fram-

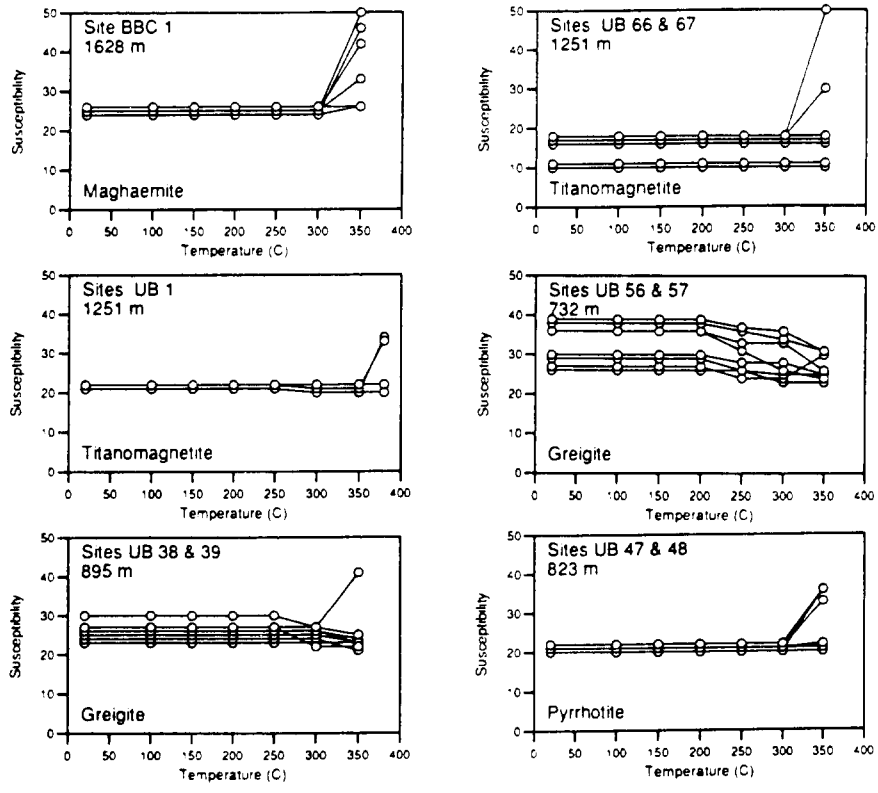

Fig. 7. Bulk susceptibility changes on thermal demagnetisation for six Upton Brook sites for which magnetic minerals have been identified. Measurements shown are volume susceptibility ($\times 10^{-6}$ SI).

boids. However, this could not be demonstrated in this study.

4.4. Thermomagnetic measurements

Only three sites yielded magnetic separates with sufficient ferrimagnetic material to enable the measurement of Curie points. Two of the separates, from fine-grained mudstone sites UB 38 & 39 and UB 56 & 57, displayed similar results (Fig. 6). Both separates were heated and cooled in air and display thermal instability between 300 and 400°C, characterised by a rapid drop in magnetisation during heating. Rather than a continued decrease in M_s, magnetisation increases above 440°C until it peaks at temperatures over 500°C; it then decreases again to zero at 580°C for UB 56 & 57 and at over 600°C for UB 38 & 39. The thermomagnetic curves for sites UB 56 & 57 and UB 38 & 39 in Fig. 6 are very similar to those obtained for greigite by other workers [22–25]. XRD results support the conclusion that greigite is the major magnetic mineral at sites UB 56 & 57 (Table 1).

The observed increase in magnetisation above 400°C is attributed to a thermally induced chemical transformation of iron-bearing clay minerals, such as chlorite, to magnetite. Chlorite is ubiquitous in sediments of the Awatere Group (Table 1) and can decompose to a spinel structure on heating [26]. In the separate from sites UB 56 & 57, the magnetisation of the resultant magnetite decays to a Curie point at 580°C and, on cooling, shows a reversibility of the magnetite portion of the thermomagnetic decay curve. A second heating of this separate (Fig. 6b) shows the straight-

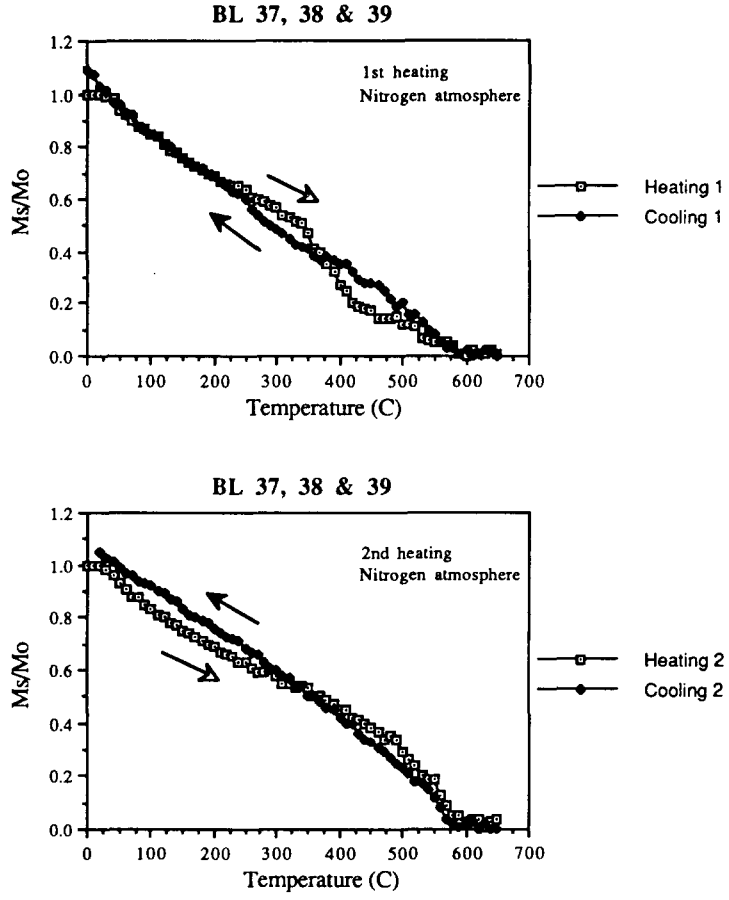

Fig. 8. Thermomagnetic curves from sites BL 37, 38 and 39. Heating and cooling cycles were done in a nitrogen atmosphere (see text).

forward decay of magnetite to its Curie point at 580°C. Non-reversibility of this curve indicates that magnetite has oxidised to haematite. The separate from sites UB 38 & 39 (Fig. 6a) displays slightly different behaviour in that the mineral produced by thermal transformation persists past the Curie point of magnetite, indicating that magnetite has oxidised to haematite, as is evident in the non-reversibility of the cooling curve.

Samples from greigite-bearing sites (UB 38 & 39 and UB 56 & 57) also display distinctly different trends of susceptibility during stepwise thermal demagnetisation (Fig. 7). Systematic decreases in susceptibility are commonly observed above temperatures of 200°C. Some samples then show an increase in susceptibility at temperatures between 300 and 350°C as is observed at most other sites. Greigite is commonly attributed with thermal instability at elevated temperatures [22,24,27–30]. Attempts to determine its thermal stability field with precision have failed because of kinetic problems associated with rate of reaction [31]. Skinner et al. [27] have shown that greigite is stable up to 238°C and that it breaks down to pyrrhotite plus sulphur vapour between 238 and 282°C, and then to pyrrhotite and pyrite at temperatures above 320°C. The observed decrease in susceptibility with heating in greigite-bearing samples (Fig. 7) indicates that a less magnetic phase begins to form at temperatures between 200 and 300°C.

Heating curves (in a nitrogen atmosphere) for a separate from sites BL 37, 38 & 39 (Fig. 8) indicate Curie points at 580°C; these curves are quasi-reversible on cooling. The first heating curve has a change in slope between 350 and 400°C, which probably defines a Curie point due to titanomagnetite. A Curie point at 580°C indicates that the final product of the heating cycle is magnetite. The second heating curve is characteristic of magnetite and is essentially reversible. The above interpretation is consistent with EPMA results that indicate the presence of titanomagnetite with inferred Curie temperatures close to 350°C.

4.5. *Isothermal remanent magnetisation*

IRM's were induced in samples from each site studied. Typical IRM acquisition curves are shown in Fig. 9. Other rock magnetic parameters are tabulated with the SIRM data in Table 2. All but one of the samples display similar behaviour (Fig. 9), with remanence saturated at fields of 200–300 mT and most values of B_{cr} near 50 mT (Table 2). Site BBC1 is the only site where saturation was

TABLE 2

Rock magnetic parameters obtained from rock magnetic experiments

Site	Stratigraphic height (m)	Lithology	Palaeomagnetic behaviour [a]	NRM (10^{-7} Am^2 kg^{-1})	SIRM (10^{-4} Am^2 kg^{-1})	B_{cr} (mT)	χ_{sp} [b] (10^{-8} m^3 kg^{-1})	SIRM/χ_{sp} (10^3 Am^{-1})
Upton Brook								
BBC1	1628	Muddy silt	6A	5.6	3.51 [c]	59	10.5	3.3 [c]
UB67	1251	Muddy sand	8B+4C	0.5	0.96	45	5.9	1.6
UB26	1016	Muddy silt	6B	0.5	0.99	62	9.0	1.1
UB39	895	Mud	10A	2.8	9.02	77	11.9	7.6
UB48	823	Muddy silt	10A	1.3	1.37	66	10.0	1.4
UB56	732	Mud	12A	7.4	9.80	75	11.1	8.8
UB58	720	Muddy silt	1A+9B+2C	0.6	0.82	66	8.7	0.9
UB64	280	Muddy silt	1A+3B+2C	1.3	0.43	52	8.2	0.5
Blind River								
BL2	1190	Muddy silt	11A	5.7	2.28	55	9.6	2.4
BL37	1105	Muddy silt	6A	5.3	3.21	57	9.8	3.3
BB4	850	Muddy silt	3A	2.4	2.21	55	9.8	2.3
BI36	172	Muddy sand	4B	4.2	1.83	49	7.2	2.5

[a] A, B and C as described in text; numerals indicate number of demagnetized samples of type A, B and C.
[b] χ_{sp} is mass specific susceptibility.
[c] Not saturated at 800 mT (value given is that at 800 mT).

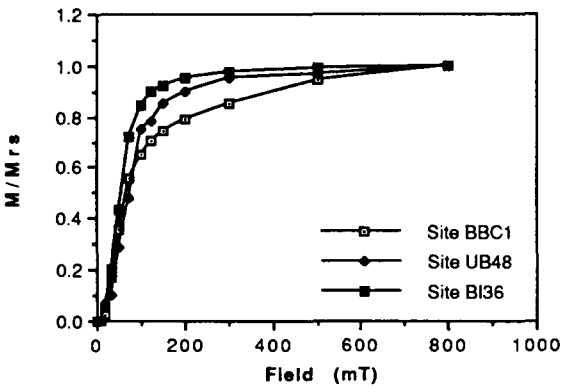

Fig. 9. Isothermal remanent magnetisation (IRM) acquisition curves for representative samples from the sites studied. Remanence becomes saturated at 300 mT for all sites except BBC1, which is still not saturated at 800 mT.

not reached by 800 mT. XRD of a magnetic separate from this site indicates the presence of maghaemite (Table 1). Lack of saturation at this site indicates the presence of an antiferromagnetic mineral, such as haematite or goethite, that was not apparent from XRD results.

Large variations exist in the rock magnetic parameters (Table 2), although patterns of magnetic behaviour are consistent. For example, B_{cr} is a sensitive indicator of grain size if mineralogy is uniform, with multidomain (*md*) grains having lower remanence coercivities than pseudo-single domain (*psd*) or stable single domain (*ssd*) grains [18]. B_{cr} shows distinct trends with variation in sediment grain size. At Upton Brook, samples from mud horizons have the highest values of B_{cr} of 77 and 75 mT. Samples from silt horizons have intermediate values of 59, 62, 66, 66 and 52 mT, while the only sample from a sandy site has the lowest value of 45 mT. Similar patterns are observed at Blind River where silt samples have B_{cr} values of 55, 57 and 55 mT and the only sandy sample has a value of 49 mT. These trends are probably indicative of variation in magnetic domain state as a response to variation in sediment grain size.

The ratio SIRM/χ_{sp} (Table 2; χ_{sp} = mass specific susceptibility) would also be expected to be sensitive to grain size [18], and some grain-size related clustering is evident on a plot of SIRM vs χ_{sp} (Fig. 10). However, there is also some variability in magnetic mineralogy. In particular, high values of SIRM/χ_{sp} are recorded from two fine-grained sites (UB39 and UB56; Fig. 10), where the remanence-bearing mineral is most likely to be greigite. Snowball and Thompson [21] also observed that greigite has higher values of χ, SIRM and SIRM/χ than many natural magnetite assemblages.

4.6. *Summary of analytical and rock magnetic measurements*

A summary of the most likely remanence carriers and the method by which they were identified

TABLE 3

Summary of remanence-carrying minerals and the methods by which they were identified

Site	Lithology	Palaeomagnetism	Remanence carrier	Means of identification
Upton Brook				
BBC1	Muddy silt	6A	Maghaemite	XRD
UB 66 & 67	Muddy sand	8B+4C	Titanomagnetite	EPMA
UB 1	Muddy silt	5B+1C	Titanomagnetite	EPMA
UB 26	Muddy silt	6B	?	–
UB 38 & 39	Mud	10A	Greigite	Curie balance
UB 47 & 48	Muddy silt	10A	Pyrrhotite	XRD
UB 56 & 57	Mud	12A	Greigite	Curie balance, XRD
UB 58 & 59	Muddy silt	1A+9B+2C	?	–
UB 64	Muddy silt	1A+3B+2C	?	–
Blind River				
BL 1, 2 & 3	Muddy silt	11A	?	–
BL 37, 38 & 39	Muddy silt	6A	Titanomagnetite	EPMA, Curie balance
BB 4	Muddy silt	3A	?	–
BI 36	Muddy sand	4B	?	–

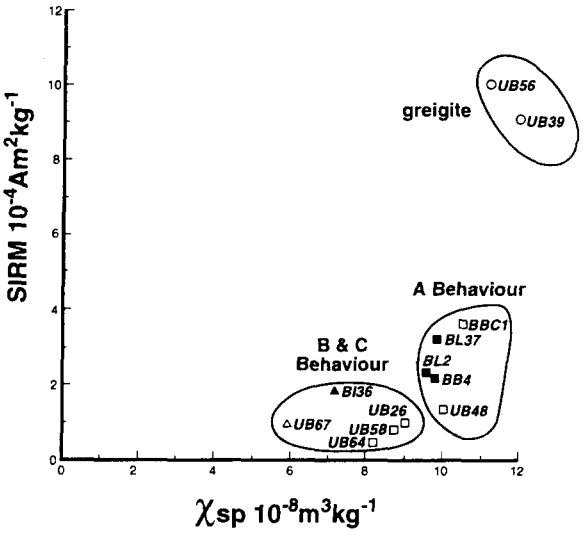

Fig. 10. SIRM vs. χ_{sp} for sites from which rock magnetic parameters were determined. Solid symbols denote Blind River sites and open symbols denote Upton Brook sites. Circles represent muds, squares represent silts and triangles represent sands.

is given for each site studied (Table 3). Ferrimagnetic iron sulphide minerals play an important role in the magnetisation of sediments at Upton Brook, with the most stable remanences being carried by greigite and pyrrhotite. Stable palaeomagnetic behaviour is also recorded at site BBC1, where maghaemite is the probable remanence carrier. The only mineral capable of carrying magnetic remanences observed at sites that are weakly and unstably magnetised is titanomagnetite, which appears to occur only in small quantities. Titanomagnetite is the only remanence-bearing mineral identified at Blind River.

5. Origin of magnetic minerals in sediments of the Awatere Group

5.1. Iron oxide minerals

Results from this study indicate that sediments of the Awatere Group contain low concentrations of titaniferous magnetite, but that ilmenite is generally common and in some cases abundant. The proportion of ilmenite in such samples is probably too high to have been derived solely from a Torlesse source, and it is likely that some opaque oxides and other heavy minerals, such as biotite and Cr-spinel, have been derived from the numerous sources of igneous rocks in central Marlborough (Fig. 1).

Titaniferous magnetite, ilmenite and other Ti-rich minerals are common throughout the igneous rocks of central Marlborough, with titanomagnetite and ilmenite occurring in approximately equal proportions and comprising up to 5% of some of these rocks [13]. However, in the Awatere Group, ilmenite occurs in much greater abundances than titanomagnetite. The few titanomagnetite grains observed in this study are generally much smaller than ilmenite grains. Dominance of ilmenite over magnetite in Torlesse rocks has also been observed by Smale [12], who showed that heavy mineral fractions with high pyrite contents (i.e. 15–30%) tend to have low ilmenite and magnetite contents. Smale [12] concluded that diagenesis may have caused solution and pyritisation of iron oxides. Dominance of ilmenite over magnetite in Awatere Group sediments is unlikely to be due to preferential mechanical breakdown of magnetite with respect to ilmenite during transportation from source, because magnetite is harder than ilmenite [26]. It is more likely that ilmenite is chemically less reactive and that titanomagnetite has been lost from the system either by oxidation during transportation or by chemical alteration due to authigenic and/or diagenetic processes, once deposited. The most likely explanation is that titanomagnetite is dissolved during early diagenesis, resulting in the formation of iron sulphide minerals, as discussed below.

5.2. Iron sulphide minerals

The relative proportion, texture and mode of occurrence of the iron sulphide minerals observed in the Awatere Group are indicative of growth in a sedimentary environment rather than a detrital origin. All iron sulphides observed occur in framboidal form and are generally associated with degraded organic structures such as microfossils. A detrital origin is also improbable because pyrite is chemically and physically unstable during the typical conditions of transport and deposition [29].

Formation of iron sulphides in sediments is a common and relatively well understood sedimentary process [29,30,32,33]. Most marine sediments

and sedimentary rocks contain at least traces of pyrite because a major proportion of the world's mud is, and was, buried under anoxic, sulphate reducing conditions [33]. Pyrite is the most stable iron mineral under reducing conditions [29] and there is a well-defined chemical pathway by which it is formed [29,30,32–34]. This pathway involves the formation of intermediate ferrimagnetic iron sulphides, such as pyrrhotite and greigite, before formation of the paramagnetic final product, pyrite. Because this pathway is of relevance to the present discussion, the principal steps in the process of sedimentary pyrite formation are detailed below.

Detrital iron minerals are by far the chief source of iron for pyrite formation in most sediments because natural surface waters contain almost no dissolved iron. Iron minerals can be decomposed to form soluble ferrous ions by bacterial or inorganic processes in anaerobic envi-

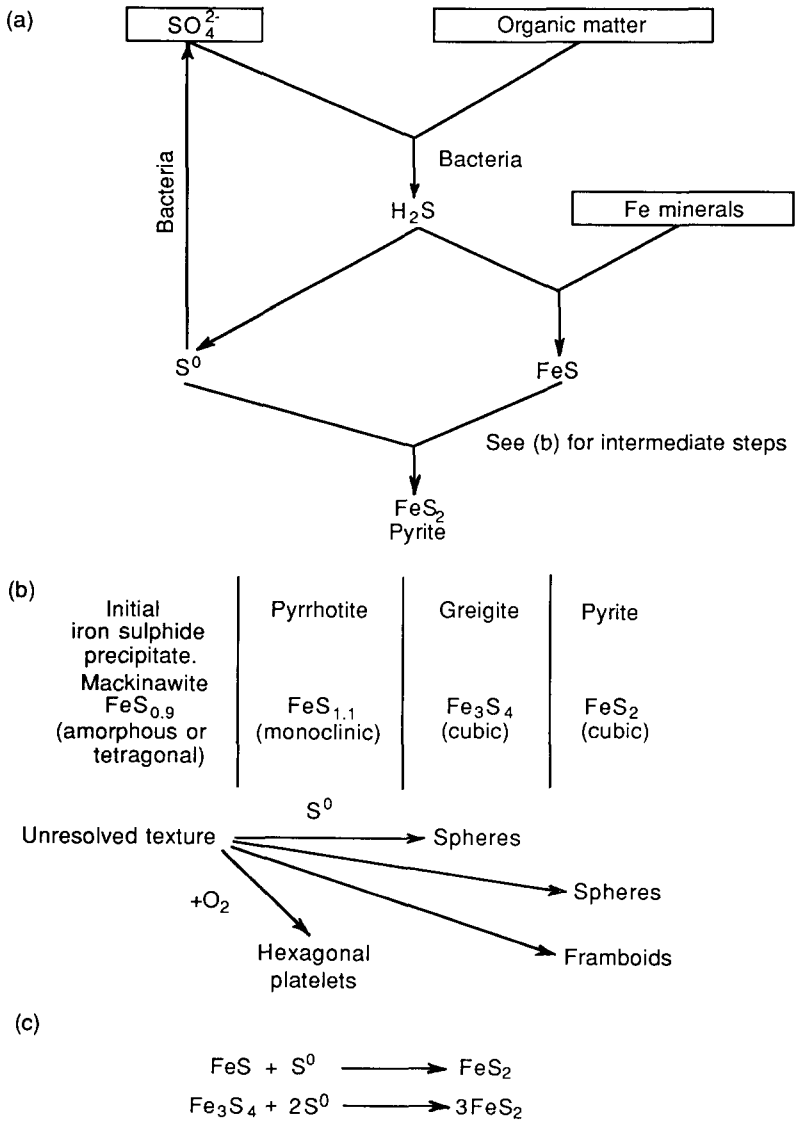

Fig. 11. Sedimentary pyrite formation: (a) Diagrammatic representation of the pyrite formation process, after Berner [33]. (b) Schematic presentation of results of textures developed during sulphurisation reactions, after Sweeney and Kaplan [30]. (c) Chemical equations of sulphurisation reactions, after Berner [29].

ronments. Pyrite forms during shallow burial as a result of the reaction of ferrous ions with H_2S. The most important source of H_2S is the reduction of interstitial dissolved sulphate by bacteria that use sedimentary organic matter as a reducing agent and energy source (Fig. 11a).

Three principal factors limit the amount of iron sulphide that can form in a sediment: the availability of dissolved sulphate, the concentration of organic compounds that can be utilised by sulphate-reducing bacteria to produce H_2S, and the concentration and reactivity of iron compounds [33]. The first step in the process is the bacterial reduction of sulphate, which can occur only under anoxic conditions. In normal marine conditions, bottom waters contain dissolved oxygen, but anoxic conditions arise in most subaqueous sediments because all dissolved oxygen near the sediment–water interface is rapidly consumed by oxic bacteria that use oxygen to convert organic matter to CO_2. Anoxic conditions necessary for bacterial sulphate reduction therefore normally occur below a depth of a few centimetres. The major factor that controls the rate of bacterial sulphate reduction in normal marine sediments is the amount and reactivity of organic matter deposited in the sediment. Westrich and Berner [35] showed that sulphate reduction rates diminish to zero at depths greater than 1 m in modern sediments from Long Island Sound, Connecticut, due almost entirely to the progressive consumption of reactive organic compounds during burial. Sulphide formation is also limited by the amount and reactivity of detrital iron minerals in the sediment. Iron minerals are usually sufficiently abundant and reactive in terrigenous sediments deposited under normal marine conditions that this factor does not pose a serious problem. The higher the H_2S concentration in pore waters, and the longer it is maintained, the greater will be the amount of detrital iron compounds transformed to pyrite.

Pyrite is not formed as a direct product of this reaction, but as the end product after a series of other metastable iron sulphides have crystallised (Fig. 11b). Berner [36] observed that the first iron sulphide formed from aqueous solution is the most sulphur deficient of the series, with a composition similar to that of mackinawite ($FeS_{0.9}$). Sweeney and Kaplan [30] observed that, in the presence of limited oxygen, the first product may react to form hexagonal pyrrhotite. Further reaction of either of these phases with elemental sulphur will produce greigite and finally pyrite (Fig. 11b). Mackinawite and greigite are thermodynamically metastable relative to pyrite and it would thus be expected that mackinawite and greigite should disappear during diagenesis by reacting to form pyrite [29]. Greigite is, however, being frequently identified in recent studies of ancient sediments that have undergone diagenesis [25,27,37–40, this study]. It is therefore possible that greigite-bearing sediments represent an arrested stage of diagenesis brought about by a paucity of H_2S [29].

In this study pyrite is observed to have formed in sediments with appreciable silt and sand contents. It is inferred that the diagenetic conditions in these sediments were such that the iron sulphide formation pathway progressed all the way to pyrite and that only traces of intermediate sulphide phases remain. Widespread preservation of intermediate sulphide phases, such as greigite and pyrrhotite, seems to have occurred only in fine-grained sediments comprising purely mud. It is inferred that, in this situation, diagenetic pyrite formation was arrested because of the low permeability of the massive mud, resulting in the consumption of available H_2S before full reaction to pyrite could occur. Greater permeability in coarser grained sediments would enable penetration of sulphate-rich pore fluids to complete the pyritisation process. Sediment grain size and permeability may therefore be important limiting factors in the formation of iron sulphides in the Awatere Group. Restriction of pyritisation is clearly conducive to the formation of stable and intense magnetisations in these mudstones.

Pyritisation also has an important effect on the magnetisation recorded in coarser grained rocks because detrital iron oxides are likely to have been dissolved during pyrite formation. Ample evidence is accumulating that suggests that the alteration of primary magnetite and subsequent formation of iron sulphides during early diagenesis is a common cause of magnetic instability in marine sediments [41–48]. Karlin and Levi [44] showed that dramatic downcore decreases in intensity of NRM, ARM, IRM and magnetic stability, accompanied by systematic increases in pyrite

content, occur in marine sediments from the eastern Pacific Ocean. These changes are claimed to be due to reduction and dissolution of ferrimagnetic iron oxides with depth during early diagenesis. Karlin and Levi [44] and Karlin [48] believe that the palaeomagnetic directional signal can survive diagenetic dissolution if detrital magnetic particles are stable and occur in sufficient concentrations.

Canfield and Berner [45] state that magnetite dissolution should be ubiquitous in sediments supporting active sulphate reduction and H_2S formation. Dissolution will vary in degree according to the surface area of the magnetite grain, concentration of dissolved sulphate and the time that magnetite is in contact with sulphate-rich pore fluids, which in turn depend on sedimentation rate, sulphate reduction rate, depth and intensity of bioturbation and reactivity of iron minerals contained in the sediment [45]. Magnetite preservation is thus favoured by rapid sedimentation, combined with high concentrations of reactive iron.

Sulphate reduction and H_2S formation must have occurred in the Awatere Group because iron sulphides are ubiquitous. Dissolution of titanomagnetite is therefore highly likely according to the evidence compiled by Canfield and Berner [45]. This contention is supported by the observation that in Awatere Group sediments containing significant pyrite, titanomagnetite grains are generally small and relatively sparse compared to ilmenite grains. If these Fe-Ti oxides are derived from a central Marlborough igneous source, ilmenite and titanomagnetite should occur in approximately equal proportions [13]. That they do not suggests that titanomagnetite is more reactive than ilmenite under such conditions. Low intensities of magnetisation can be explained by the low proportion of titanomagnetite due to the diagenetic dissolution of a large proportion of detrital titanomagnetite grains. Preservation of some titanomagnetite is likely to be the result of high sedimentation rates of the order of 0.5 m/k.y. [5,8,10] and high concentrations of reactive iron. Stable characteristic palaeomagnetic directions are often discernible despite dissolution of the remanence carriers. Relative palaeomagnetic instability and weak remanence intensities in sediments containing grains that are silt sized and larger may therefore be due to low titanomagnetite concentrations resulting from pyritisation and titanomagnetite dissolution.

If the stable characteristic magnetisations carried by sulphide minerals (Fig. 3) are acquired during early diagenesis, it is important to establish an estimate of the time lag between sediment deposition and acquisition of magnetisation before palaeomagnetic data can be interpreted with confidence. The results of Westrich and Berner [35] and Canfield and Berner [45] indicate that sulphide formation is severely restricted below the surface metre of marine sediments. If so, iron sulphides will form during early diagenesis, within 2000 years of deposition for sediments deposited at rates > 0.5 m/k.y. Such a lag between deposition and acquisition of remanence is insignificant compared to the resolution of the geomagnetic polarity timescale and is therefore acceptable for magnetostratigraphic purposes. Studies of shorter period geomagnetic fluctuations, such as palaeosecular variation or geomagnetic polarity transitions, are more seriously affected by such a time lag, particularly if the rate of remanence acquisition is substantially different from the sedimentation rate, or if there are several carriers which have their remanence locked in at different times [e.g. 49,50).

Some cases exist where dissolved sulphate occurs at depth, giving rise to iron sulphides during late diagenesis. In these cases, sulphate is derived from hydrocarbon seepage [40] and deeper evaporite deposits [46]. Such conditions certainly do not exist in the Awatere Group; thus the most likely time for sulphide formation is during burial at depths of < 1 m, while dissolved sulphate is available to react with soluble iron compounds.

6. Conclusions

Results of rock magnetic experiments and mineralogical studies of magnetic separates indicate that the ferrimagnetic iron sulphides, greigite and pyrrhotite, are the major contributors to the stable remanences recorded in fine-grained sediments of the Awatere Group where early diagenetic pyritisation has been arrested. Detrital ferrimagnetic iron oxides are apparently the major contributors where pyritisation has progressed to completion. Pyritisation has almost certainly

caused dissolution of detrital titanomagnetite grains during early diagenesis. Clearly, understanding of diagenetic processes in such sediments is vital to the understanding of the magnetisation process and the interpretation of palaeomagnetic data.

Acknowledgements

Financial support was provided by the New Zealand University Grants Committee, the Victoria University Internal Research Committee, and the Institute of Geophysics, Victoria University of Wellington, New Zealand. We are grateful to Dr Carlo Laj for use of facilites at the C.F.R. palaeomagnetic laboratory, Gif-sur-Yvette, France. Drs Emanuel Tric and Piotr Tucholka were particularly helpful in their assistance to this study. Electron microprobe analyses were made by Joel Baker and Ken Palmer at the Analytical Facility, Research School of Earth Sciences, Victoria University. We thank Profs Paul Vella and Rob Van der Voo for their criticisms of earlier versions of the manuscript.

References

1 K.L. Verosub, Depositional and postdepositional processes in the magnetization of sediments, Rev. Geophys. Space Phys. 15, 129–143, 1977.
2 S.K. Banerjee, Problems and current trends in rock magnetism and paleomagnetism, Eos Trans. Am. Geophys. Union 68(30), 650 and 662–663, 1987.
3 J.P. Kennett, N.D. Watkins and P.P. Vella, Paleomagnetic chronology of Pliocene–Early Pleistocene climates and the Plio-Pleistocene boundary in New Zealand, Science 171, 272–274, 1971.
4 B.R. Lienert, D.A. Christoffel and P.P. Vella, Geomagnetic dates on a New Zealand Upper Miocene–Pliocene section, Earth Planet. Sci. Lett. 16, 195–199, 1972.
5 J.P. Kennett and N.D. Watkins, Late Miocene–Early Pliocene paleomagnetic stratigraphy, paleoclimatology and biostratigraphy in New Zealand, Bull. Geol. Soc. Am. 85, 1385–1398, 1974.
6 D. Seward, D.A. Christoffel and B.R. Lienert, Magnetic polarity stratigraphy of a Plio-Pleistocene marine sequence of North Island, New Zealand, Earth Planet. Sci. Lett. 80, 353–360, 1986.
7 I.C. Wright and P.P. Vella, A New Zealand Late Miocene magnetostratigraphy: glacioeustatic and biostratigraphic correlations, Earth Planet. Sci. Lett. 87, 193–204, 1988.
8 G.M. Turner, A.P. Roberts, C. Laj, C. Kissel, A. Mazaud, S. Guitton and D.A. Christoffel, New paleomagnetic results from Blind River: revised magnetostratigraphy and tectonic rotation of the Marlborough region, South Island, New Zealand, N.Z. J. Geol. Geophys. 32, 191–196, 1989.
9 D.M. McGuire, Paleomagnetic stratigraphy and magnetic properties of Pliocene strata, Turakina River, North Island, New Zealand, Ph.D. Thesis, Victoria Univ., Wellington, 1989 (Unpubl.).
10 A.P. Roberts, Cainozoic palaeomagnetism and tectonics of the Marlborough region, South Island, New Zealand, Ph.D. Thesis, Victoria Univ., Wellington, 1990 (Unpubl.).
11 G.M. Turner and P.J.J. Kamp, Palaeomagnetic location of the Jaramillo and the Matuyama–Brunhes transition in the Castlecliffian stratotype section, Wanganui Basin, New Zealand, Earth Planet. Sci. Lett. 100, 42–50, 1990.
12 D. Smale, Heavy minerals in Cretaceous sandstones in Marlborough, N.Z. Geol. Surv. Rep. SL14.
13 R.H. Grapes, Petrology of the Blue Mountain Igneous Complex, Marlborough, New Zealand, J. Petrol. 16, 371–428, 1975.
14 A.P. Roberts and G.S. Wilson, Stratigraphy of the Awatere Group, Marlborough, New Zealand, J. R. Soc. N.Z. 22, 187–204, 1992.
15 S. Papamarinopoulos, P.W. Readman, Y. Maniatus and A. Simopoulos, Magnetic characterisation and Mossbauer spectroscopy of magnetic concentrates from Greek lake sediments, Earth Planet. Sci. Lett. 57, 173–181, 1982.
16 M.J. Dekkers, Some rock magnetic parameters for natural goethite, pyrrhotite and fine-grained hematite, Ph.D. Thesis, State Univ. Utrecht, 1988 (Unpubl.)
17 I. Snowball and R. Thompson, The occurrence of greigite in sediments from Loch Lomond, J. Quat. Sci. 3, 121–125, 1988.
18 R. Thompson and F. Oldfield, Environmental Magnetism, Allen & Unwin, London, 1986.
19 J.C. Stormer, The effects of recalculation on estimates of temperature and oxygen fugacity from analyses of multicomponent iron–titanium oxides, Am. Mineral. 68, 586–594, 1983.
20 C.N. Keefer and P.N. Shive, Curie temperature and lattice constant reference contours for synthetic titanomaghemites, J. Geophys. Res. 86, 987–998, 1981.
21 M. Farrand, Framboidal sulphides precipitated synthetically, Miner. Deposita 5, 237–247, 1970.
22 I. Snowball and R. Thompson, A stable chemical remanence in Holocene sediments, J. Geophys. Res. 95, 4471–4479, 1990.
23 I. Snowball and R. Thompson, A mineral magnetic study of Holocene sedimentation in Lough Catherine, Northern Ireland, Boreas 19, 127–146, 1990.
24 I. Snowball, Magnetic hysteresis properties of greigite (Fe_3S_4) and a new occurrence in Holocene sediments from Swedish Lappland, Phys. Earth Planet. Inter. 68, 32–40, 1991.
25 E. Tric, C. Laj, C. Jehanno, J.-P. Valet, C. Kissel, A. Mazaud and S. Iaccarino, High-resolution record of the Upper Olduvai transition from Po Valley (Italy) sediments: support for dipolar transition geometry?, Phys. Earth Planet. Inter. 65, 319–336, 1991.
26 W.A. Deer, R.A. Howie and J. Zussman, An Introduction to the Rock Forming Minerals, Longman, 1966.
27 B.J. Skinner, R.C. Erd and F.S. Grimaldi, Greigite, the

thio-spinel of iron; a new mineral, Am. Mineral. 49, 543–555, 1964.
28 R.A. Berner, Thermodynamic stability of sedimentary iron sulfides, Am. J. Sci. 265, 773–785, 1967.
29 R.A. Berner, Principles of Chemical Sedimentology, McGraw-Hill, New York, 1971.
30 R.E. Sweeney and I.R. Kaplan, Pyrite framboid formation. Laboratory synthesis and marine sediments, Econ. Geol. 68, 618–634, 1973.
31 J.R. Craig and S.D. Scott, Sulfide phase equilibria, In: Sulfide Mineralogy, P.H. Ribbe, ed., Mineral. Soc. Am. Short Course Notes 1, CS1–CS110, 1974.
32 R.A. Berner, Sedimentary pyrite formation, Am. J. Sci. 268, 1–23, 1970.
33 R.A. Berner, Sedimentary pyrite formation: an update, Geochim. Cosmochim. Acta 48, 605–615, 1984.
34 B.F. Jones and C.J. Bowser, The mineralogy and related chemistry of lake sediments, In: Lakes: Chemistry, Geology, Physics, A. Lerman, ed., pp. 179–227, Springer, New York, 1978.
35 J.T. Westrich and R.A. Berner, The role of sedimentary organic matter in bacterial sulfate reduction: the G model tested, Limnol. Oceanogr. 29, 236–249, 1984.
36 R.A. Berner, Iron sulfides formed from aqueous solution at low temperatures and atmospheric pressure, J. Geol. 72, 293–306, 1964.
37 C.S. Horng, Study of magnetic minerals and magnetostratigraphy of the Tsengwenchi and Erhjenchi sections, southwestern Taiwan, Ph.D. Thesis, National Taiwan Univ., Taipei, 1991 (Unpubl.).
38 V. Kalcheva, P. Nozharov, M. Kovacheva and V. Shopov, Paleomagnetic research on Black Sea Quaternary sediments, Phys. Earth Planet. Inter. 63, 113–120, 1990.
39 M. Krs, M. Krsova, P. Pruner, A. Zeman, F. Novak and J. Jansa, A petromagnetic study of Miocene rocks bearing micro-organic material and the magnetic mineral greigite (Sokolov and Cheb basins, Czechoslovakia), Phys. Earth Planet. Inter. 63, 98–112, 1990.
40 R.L. Reynolds, N.S. Fishman and M.R. Hudson, Sources of aeromagnetic anomalies over Cement Oil Field (Oklahoma), Simpson Oil Field (Alaska), and the Wyoming–Idaho–Utah Thrust Belt, Geophysics 56, 606–617, 1991.
41 K. Kobayashi and M. Nomura, Iron sulphides in the sediment cores from the Sea of Japan and their geophysical implications, Earth Planet. Sci. Lett. 16, 200–208, 1972.
42 D.V. Kent and W. Lowrie, Origin of magnetic instability in sediment cores from central North Pacific, J. Geophys. Res. 79, 2987–3000, 1974.
43 P.C. Henshaw and R.T. Merrill, Magnetic and chemical changes in marine sediments, Rev. Geophys. Space Phys. 18, 483–504, 1980.
44 R. Karlin and S. Levi, Geochemical and sedimentological control of the magnetic properties of hemipelagic sediments, J. Geophys. Res. 90, 10373–10392, 1985.
45 D.E. Canfield and R.A. Berner, Dissolution and pyritization of magnetite in anoxic marine sediments, Geochim. Cosmochim Acta 51, 645–659, 1987.
46 J.E.T. Channell and T. Hawthorne, Progressive dissolution of titanomagnetites at ODP Site 653 (Tyrrhenian Sea), Earth Planet. Sci. Lett. 96, 469–480, 1990.
47 B.W. Leslie, S.P. Lund and D.E. Hammond, Rock magnetic evidence for the dissolution and authigenic growth of magnetic minerals within anoxic marine sediments of the California continental borderland, J. Geophys. Res. 95, 4437–4452, 1990.
48 R. Karlin, Magnetite diagenesis in marine sediments from the Oregon continental margin, J. Geophys. Res. 95, 4405–4419, 1990.
49 A.A.M. Van Hoof and C.G. Langereis, Reversal records in marine marls and delayed acquisition of remanent magnetization, Nature 351, 223–225, 1991.
50 A.A.M. Van Hoof and C.G. Langereis, The Upper Kaena sedimentary geomagnetic reversal record from southern Sicily, J. Geophys. Res. 97, 6941–6957, 1992.